ISSN 1064-2269, Journal of Communications Technology and Electronics, 2019, Vol. 64, No. 7, pp. 664–674.

ELECTRODYNAMICS
AND WAVE PROPAGATION

Scattering of Electromagnetic Waves on a Subwave Lattice of Square Strip Conductors

B. A. Belyaev[a, b, *], **V. V. Tyurnev**[a, b], **and N. V. Volkov**[a, c]

[a] *Kirensky Institute of Physics, KSC Federal Research Center, Siberian Branch, Russian Academy of Sciences, Krasnoyarsk, 660036 Russia*

[b] *Siberian Federal University, Krasnoyarsk, 660041 Russia*

[c] *Reshetnev Siberian State University of Science and Technology, Krasnoyarsk, 660014 Russia*

**e-mail: belyaev@iph.krasn.ru*

Received June 13, 2018; revised October 5, 2018; accepted October 5, 2018

Abstract—Simple formulas are obtained for calculating the scattering matrix of a plane electromagnetic wave incident normally on an infinite 2D lattice formed by square strip conductors and located at the interface of two dielectric media. For the first time, the vortex behavior of the electric field of the lattice was taken into account, which made it possible to repeatedly reduce the computation error at high frequencies. This is confirmed by the close agreement of the amplitude-frequency responses of the structure calculated by the formulas with the characteristics obtained by the numerical electrodynamic analysis of the 3D model when the lattice period is less than half the wavelength.

DOI: 10.1134/S1064226919070039

INTRODUCTION

As is known, multilayer thin-film dielectric mirrors are widely used in optics due to their high reflectance. The possibility of varying the reflectivity of such mirrors by changing the contrast of the dielectric constant and the number of layers [1] allows us to use them in band-pass filters (BPF) as the coupling elements between the resonators forming the bandwidth, as well as the coupling elements of the terminal resonators with the surrounding space [2]. However, such filters are difficult to manufacture and, as a rule, have a large non-uniformity of the amplitude-frequency response (AFR) in the passband when the filter order is higher than the second order. The known methods for reducing the non-uniformity of the frequency response in the passband of multilayer dielectric filters [3–5] do not reduce the complexity of their manufacture. Therefore, the search for and study of new approaches for designing BPFs on layered structures is an important and urgent task.

At present, many researchers use designs based on dielectric layers on the surface of which resonant 2D structures are made of metal conductors, the so-called frequency selective surfaces, to create filters. Such constructions serve as BPFs and band-stop filters in the ranges from micron [6–8] to decimeter [9–11] wavelengths. We note an important feature of frequency-selective surfaces, which lies in the fact that their frequency characteristics depend on the angle of incidence and polarization of the electromagnetic wave [12].

The first frequency-selective surfaces were flat two-dimensionally periodic metal lattices, the elementary cells of which were made both as rectangular holes in a thin metal screen (grids) and thin flat rectangular conductors located on a dielectric substrate [13]. The size of the unit cell of the lattice is approximately equal to the wavelength at the resonant frequency. The cascading of several such metal resonant lattices allows us to create multilayer structures, the frequency response of which corresponds to a high-order BPF [12]. However, flat metal lattices containing resonant elementary cells have a low self-Q because of the high ohmic losses in the conductors.

Therefore, the designs of frequency selective surfaces, in which, as in traditional optical filters [12], half-wave dielectric layers are resonators, are more promising. However, instead of multilayer dielectric mirrors, they use the nonresonant subwave wave lattices of the strip conductors located at the interfaces of the dielectric resonator layers. Such lattices, in particular, can be 1D-lattices of ribbon strip conductors with a period much shorter than the wavelength, having a parallel direction of the axes of symmetry on all layers [14, 15]. An electrodynamic analysis of such tape strip structures is presented in [16, 17]. Filters on dielectric layers, the mirrors of which are tape strip structures with parallel axes, have frequency selective properties only for electromagnetic waves with linear polarization and the direction of the electric field vector along the strip lines. Such filters pass orthogonal polarization waves with low losses in the frequency range from zero and above.

The resonators in the construction of the filters under consideration can consist not of one but of two dielectric layers, also separated by a subwave 1D lattice of stripline conductors, but with the orthogonal axis with respect to 1D lattices at the boundaries of two-layer resonators [18]. Such a filter is also a polarizer. In the given frequency band, it transmits waves of linear polarization with the direction of the electric field vector along the outer strip conductors; however, it barely transmits waves of orthogonal polarization [18].

The filter in which sub-wave metal grids with square windows are used as mirrors at the boundaries of the dielectric resonator layers does not exhibit polarization properties. In the work [19], an experimental sample of a third-order filter with grids between dielectric layers, possessing not only high characteristics but also good agreement of the frequency response of the measured and the frequency response calculated by the numerical electrodynamic analysis of a 3D model of the device, was investigated. However, the electrodynamic analysis programs of such complex structures require significant machine time; therefore, the parametric synthesis of the filter was carried out by the speed matrix method using the formulas obtained in [20], which describe the reflective properties of the metal grids quite well. The design parameters found as a result of the synthesis were used as the initial parameters in parametric synthesis using the electrodynamic analysis of the 3D model.

For grids of square strip conductors, which can also serve as mirrors in filters on dielectric resonator layers, similar formulas describing their reflective properties have not yet been obtained. In calculations of a grid of strip conductors, formulas are usually used for the scattering matrix of electromagnetic waves of linear polarization on the corresponding grid of parallel ribbon conductors [13, 21] with the same period and width when the electric field vector is orthogonal to the direction of the conductors. Obviously, with this approach, the elements of the scattering matrix describe only the capacitive interactions of the strip conductors, but the inductive interactions are completely ignored, the relative contribution of which increases in proportion to the square of the frequency.

In this paper, we calculated the scattering matrix of electromagnetic waves that are orthogonal to a flat 2D lattice of square strip conductors located at the interface of two dielectric media. In the calculation, the method of solving Maxwell's equations is used for certain selected areas of the structure under consideration, which was used in [20]. In this calculation, along with the potential part of the electric field, the vortex part is also considered, which significantly increases the accuracy of the calculation in the high-frequency region.

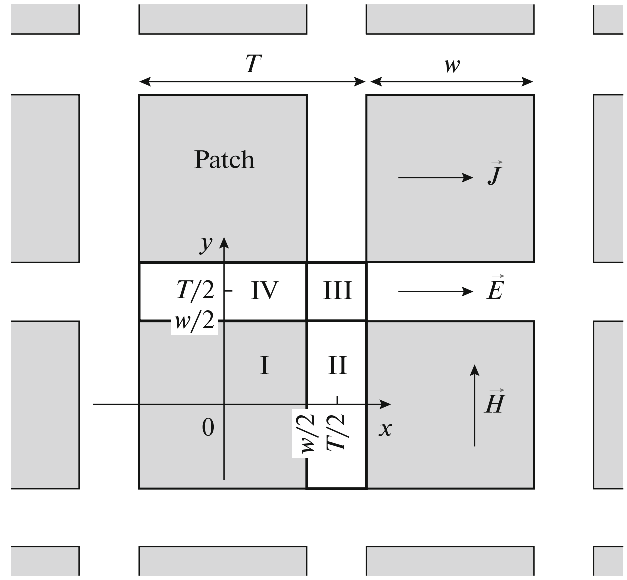

Fig. 1. Strip conductor lattice; I, II, III and IV are considered sections of its unit cell.

1. ELECTROMAGNETIC FIELD OF GRID OF SQUARE STRIP CONDUCTORS

Calculate the electromagnetic fields near the lattice of square strip conductors at the interface of two dielectric media (Fig. 1). The fields are excited by linearly polarized waves with the components normally incident on the lattice on both sides.

$$E_x^{\text{inc}} = \begin{cases} E_1^{\text{inc}} \exp(ik_1 z - i\omega t), & \text{if } z < 0, \\ E_2^{\text{inc}} \exp(-ik_2 z - i\omega t), & \text{if } z > 0, \end{cases}$$
$$H_y^{\text{inc}} = \begin{cases} Z_1^{-1} E_1^{\text{inc}} \exp(ik_1 z - i\omega t), & \text{if } z < 0, \\ -Z_2^{-1} E_2^{\text{inc}} \exp(-ik_2 z - i\omega t), & \text{if } z > 0, \end{cases} \tag{1}$$

where

$$k_{1,2} = \omega\sqrt{\varepsilon_0 \mu_0 \varepsilon_{1,2}} \tag{2}$$

are wave numbers, and

$$Z_{1,2} = Z_0 \big/ \sqrt{\varepsilon_{1,2}}, \quad Z_0 = \sqrt{\mu_0 / \varepsilon_0} \tag{3}$$

are the haracteristic resistances, subscripts 1 and 2 indicate the sides of the lattice in contact, respectively, with the medium with a dielectric constant ε_1 and with a medium with a dielectric constant ε_2. The origin of coordinates z is selected on the surface of the lattice.

Since the components of the field of incident waves (1) are homogeneous in the lattice plane, the components of the lattice field excited by them $\vec{E}^{\text{lat}}$ and $\vec{H}^{\text{lat}}$ are generally periodic functions of coordinates x and y with the period equal to the lattice period T. This means that any of the components of the electromagnetic field can be decomposed into a double Fourier series of arguments x and y. Given the symmetry of the field components relative to the lattice symmetry planes, we can write the following expansions:

$$
\begin{aligned}
E_x^{\mathrm{lat}}(x,y,z) &= \sum_{n=0}^{\infty}\sum_{m=0}^{\infty} E_x^{nm}(z)\cos(k_n x)\cos(k_m y),\\
H_y^{\mathrm{lat}}(x,y,z) &= \sum_{n=0}^{\infty}\sum_{m=0}^{\infty} H_y^{nm}(z)\cos(k_n x)\cos(k_m y),\\
E_z^{\mathrm{lat}}(x,y,z) &= \sum_{n=0}^{\infty}\sum_{m=0}^{\infty} E_z^{nm}(z)\sin(k_n x)\cos(k_m y),\\
H_z^{\mathrm{lat}}(x,y,z) &= \sum_{n=0}^{\infty}\sum_{m=0}^{\infty} H_z^{nm}(z)\cos(k_n x)\sin(k_m y),
\end{aligned}
\tag{4}
$$

where $k_n = 2\pi n/T$ and $k_m = 2\pi m/T$. We require each member of the double Fourier series in expressions (4) to satisfy the Helmholtz equations

$$\left(\partial^2/\partial x^2 + \partial^2/\partial y^2 + \partial^2/\partial z^2 + k_{1,2}^2\right)\vec{E}^{\mathrm{lat}} = 0, \tag{5}$$

$$\left(\partial^2/\partial x^2 + \partial^2/\partial y^2 + \partial^2/\partial z^2 + k_{1,2}^2\right)\vec{H}^{\mathrm{lat}} = 0. \tag{6}$$

In this case, at $z < 0$, formulas (4) take the form

$$
\begin{aligned}
E_x^{\mathrm{lat}} &= E_x^{00}\exp(ik_1|z|)\\
&+ \sum_{n=1}^{\infty}\sum_{m=1}^{\infty} E_x^{nm}\cos(k_n x)\cos(k_m y)\exp(-k_1^{nm}|z|),\\
H_y^{\mathrm{lat}} &= H_{1y}^{00}\exp(ik_1|z|)\\
&+ \sum_{n=1}^{\infty}\sum_{m=1}^{\infty} H_{1y}^{nm}\cos(k_n x)\cos(k_m y)\exp(-k_1^{nm}|z|),\\
E_z^{\mathrm{lat}} &= \sum_{n=1}^{\infty}\sum_{m=1}^{\infty} E_{1z}^{nm}\sin(k_n x)\cos(k_m y)\exp(-k_1^{nm}|z|),\\
H_z^{\mathrm{lat}} &= \sum_{n=1}^{\infty}\sum_{m=1}^{\infty} H_z^{nm}\cos(k_n x)\sin(k_m y)\exp(-k_1^{nm}|z|);
\end{aligned}
\tag{7}
$$

and at $z > 0$, they take the form

$$
\begin{aligned}
E_x^{\mathrm{lat}} &= E_x^{00}\exp(ik_2|z|)\\
&+ \sum_{n=1}^{\infty}\sum_{m=1}^{\infty} E_x^{nm}\cos(k_n x)\cos(k_m y)\exp(-k_2^{nm}|z|),\\
H_y^{\mathrm{lat}} &= H_{2y}^{00}\exp(ik_2|z|)\\
&+ \sum_{n=1}^{\infty}\sum_{m=1}^{\infty} H_{2y}^{nm}\cos(k_n x)\cos(k_m y)\exp(-k_2^{nm}|z|),\\
E_z^{\mathrm{lat}} &= \sum_{n=1}^{\infty}\sum_{m=1}^{\infty} E_{2z}^{nm}\sin(k_n x)\cos(k_m y)\exp(-k_2^{nm}|z|),\\
H_z^{\mathrm{lat}} &= \sum_{n=1}^{\infty}\sum_{m=1}^{\infty} H_z^{nm}\cos(k_n x)\sin(k_m y)\exp(-k_2^{nm}|z|),
\end{aligned}
\tag{8}
$$

where

$$k_{1,2}^{nm} = \sqrt{k_n^2 + k_m^2 - k_{1,2}^2}. \tag{9}$$

Here we have taken into account that the field components E_x^{lat} and H_z^{lat} are continuous when $z = 0$. Formulas (7) and (8) can be considered as a decomposition of the lattice field components $\vec{E}^{\mathrm{lat}}$ and $\vec{H}^{\mathrm{lat}}$ in a row in all modes corresponding to the lattice symmetry and polarization of the incident waves.

We will assume that the lattice period T is much shorter than the wavelength, i.e., $k_{1,2}T \ll 2\pi$. This allows us to perform an electrodynamic calculation in the quasi-static approximation and, instead of the Helmholtz equations (5) and (6), solve the Laplace equations

$$\left(\partial^2/\partial x^2 + \partial^2/\partial y^2 + \partial^2/\partial z^2\right)\vec{E}^{\mathrm{lat}} = 0, \tag{10}$$

$$\left(\partial^2/\partial x^2 + \partial^2/\partial y^2 + \partial^2/\partial z^2\right)\vec{H}^{\mathrm{lat}} = 0. \tag{11}$$

In this case, in expansions (7) and (8), all members of the Fourier series, except the main members with $n = m = 0$, rapidly decrease as $|z|$ increases. Therefore, formulas (7) and (8) in the far zone at $k_{1,2}|z| \gg 1$ are simplified and take the form

$$
\begin{aligned}
E_x^{\mathrm{lat}}(x,y,z) &= E_x^{00}\exp(ik_1|z|)\\
H_y^{\mathrm{lat}}(x,y,z) &= \begin{cases} H_{1y}^{00}\exp(ik_1|z|) & \text{for } z < 0\\ H_{2y}^{00}\exp(ik_2|z|) & \text{for } z > 0,\end{cases}\\
E_z^{\mathrm{lat}}(x,y,z) &= 0,\\
H_z^{\mathrm{lat}}(x,y,z) &= 0,
\end{aligned}
\tag{12}
$$

where the amplitudes of the field components are expressed by the integrals

$$E_x^{00} = \frac{1}{T^2}\int\limits_{x=-w/2}^{T-w/2}\int\limits_{y=-w/2}^{T-w/2} E_x^{\mathrm{lat}}(x,y,0)\,dxdy, \tag{13}$$

$$
\begin{aligned}
H_{1y}^{00} &= \frac{1}{T^2}\int\limits_{x=-w/2}^{T-w/2}\int\limits_{y=-w/2}^{T-w/2} H_y^{\mathrm{lat}}(x,y,0)\,dxdy \quad \text{for } z < 0,\\
H_{2y}^{00} &= \frac{1}{T^2}\int\limits_{x=-w/2}^{T-w/2}\int\limits_{y=-w/2}^{T-w/2} H_y^{\mathrm{lat}}(x,y,0)\,dxdy \quad \text{for } z > 0.
\end{aligned}
\tag{14}
$$

Here w is the size of the side of the square strip conductor in the lattice. Obviously by finding the magnitude E_x^{00}, H_{1y}^{00}, and H_{2y}^{00}, we can calculate the elements of the desired scattering matrix **S** for the far zone of the lattice under consideration.

To find amplitudes E_x^{00}, H_{1y}^{00}, and H_{2y}^{00} according to formulas (13) and (14), we need to obtain solutions of the Maxwell equations only near the surface of the grid conductors. We write the boundary conditions which these solutions must satisfy. For this, it is convenient to divide the surface of the unit cell of the lattice into four rectangular regions I–IV (Fig. 1). Then, in region I, which occupies a quarter of the area of the strip conductor, the boundary conditions have the form

$$E_x^{\text{lat}}(x,y,0) = 0, \quad E_y^{\text{lat}}(x,y,0) = 0, \\ H_z^{\text{lat}}(x,y,0) = 0, \tag{15}$$

and in regions II, III, and IV, free from metallization, apart from the continuity conditions, there are no other restrictions on the components of the electromagnetic field.

Maxwell's equations for the electromagnetic field in the near-surface region of the lattice have two solutions that satisfy the boundary conditions (15). The first quasi-static solution is trivial. In the static limit, it has a single magnetic component, H_0, independent of the coordinates and directed along the magnetic field vector of the incident wave, i.e., along axis y. In the first solution, the electric field $\vec{E}^{\text{lat}}$ exists only in dynamics; it is vortex and vanishes on the entire surface of the lattice.

The second quasi-static solution has only the components of the electric field in the static limit $\vec{E}^{\text{lat}}$. It contains only the potential part $\vec{E}^{\text{pot}}$. The magnetic field $\vec{H}^{\text{lat}}$ in the second solution appears only in dynamics. It is a vortex, as it is connected with the electric field $\vec{E}^{\text{lat}}$ by Maxwell's equation

$$\text{curl}\vec{H}_{1,2}^{\text{lat}} = -i\omega\varepsilon_0\varepsilon_{1,2}\vec{E}_{1,2}^{\text{lat}}. \tag{16}$$

Therefore, in the future, the magnetic field of the second solution will be denoted as $\vec{H}_{1,2}^{\text{vort}}$. The electric field in this case should be represented by the sum

$$\vec{E}^{\text{lat}} = \vec{E}^{\text{pot}} + \vec{E}^{\text{vort}}, \tag{17}$$

where $\vec{E}^{\text{pot}}$ is the potential part of the electric field and $\vec{E}^{\text{vort}}$ is the swirl part. The potential part of the electric field is conveniently described by the scalar potential φ using equation

$$\vec{E}^{\text{pot}} = -\operatorname{grad}\varphi. \tag{18}$$

The surface of each strip conductor, together with the plane of symmetry intersecting it, orthogonal to axis x, is equipotential. This follows from the boundary conditions (15) and from the symmetry of the problem. Assuming that the potential difference φ between adjacent conductors equals U, according to formula (13) find the magnitude of the contribution to the amplitude E_x^{00} from the potential part of the electric field E_x^{pot}

$$\left\langle E_x^{\text{pot}} \right\rangle_{TT} = U/T. \tag{19}$$

Here, the subscript TT indicates that averaging E_x^{pot} was carried out by the area of the lattice unit cell with period T.

The potential part $\vec{E}^{\text{pot}}$ of the electric field is associated with surface charges ρ on strip conductors by the boundary condition

$$\varepsilon_0\varepsilon_2 E_{2z}^{\text{pot}} - \varepsilon_0\varepsilon_1 E_{1z}^{\text{pot}} = \rho. \tag{20}$$

In turn charges ρ connected to surface currents $\vec{J}$ by the conservation law

$$\operatorname{div}\vec{J} = i\omega\rho, \tag{21}$$

and the surface currents $\vec{J}$ are associated with the vortex magnetic field $\vec{H}^{\text{vort}}$ on both sides of the lattice by the boundary condition

$$H_{2x}^{\text{vort}} - H_{1x}^{\text{vort}} = J_y, \quad H_{2y}^{\text{vort}} - H_{1y}^{\text{vort}} = -J_x. \tag{22}$$

Since the magnetic field $\vec{H}^{\text{vort}}$ is vortex, its tangential components change sign when switching from one side of the strip conductor to the other side. Therefore, the boundary conditions (22) can be rewritten as

$$2H_{2x}^{\text{vort}} = J_y, \quad 2H_{2y}^{\text{vort}} = -J_x. \tag{23}$$

Find the amplitude of the magnetic field H_{2y}^{00}. From formulas (14) and (23) we get

$$H_{2y}^{00} = -\frac{1}{2T}\int\limits_{x=-w/2}^{T-w/2} \left\langle J_x(x) \right\rangle_T dx, \tag{24}$$

where

$$\left\langle J_x(x) \right\rangle_T = \frac{1}{T}\int\limits_{y=-w/2}^{T-w/2} J_x(x,y)dy \tag{25}$$

is averaged over the coordinate y density function of the longitudinal surface current. This function, according to Eq. (21) is associated with the averaged density function of surface charges

$$\left\langle \rho(x) \right\rangle_T = \frac{1}{T}\int\limits_{y=-w/2}^{T-w/2} \rho(x,y)dy \tag{26}$$

by the equality

$$\frac{\partial}{\partial x}\left\langle J_x(x) \right\rangle_T = i\omega\left\langle \rho(x) \right\rangle_T. \tag{27}$$

Here it was taken into account that the average function of the transverse current density is $\left\langle J_y(x) \right\rangle_T = 0$. When calculating the averaged charge density function $\left\langle \rho(x) \right\rangle_T$, we need to take into account the fact that the surface electric charges $\rho(x, y)$ are concentrated not only near the edge of the strip conductor facing region II but also near the other edge facing region IV. Those charges that are concentrated on the edge of the conductor facing region IV generate the component E_x^{pot} not only in areas I and II but also in areas IV and III. This is why averaging $\rho(x, y)$ by coordinate y should be carried out in areas I and IV, i.e., throughout period T.

Potential $\varphi(x, z)$, corresponding to the average function $\langle\rho(x)\rangle_T$ and potential differences U is expressed by the formula

$$\varphi(x,z) = \frac{U}{\pi}\operatorname{Im}\operatorname{arccosh}\left(\cos(\pi\frac{x+iz}{T})\Big/\cos\left(\frac{\pi w}{2T}\right)\right). \quad (28)$$

Formula (28) is an exact solution of the 2D Laplace equation for the quasi-static potential of a strip of conductors [16]. This potential is constant on the surface of the lattice at $|x| < w/2$ and with $|x-T| < w/2$.

By formulas (18) and (28), we find the normal component of the potential part of the electric field on the upper side of the lattice

$$\left\langle E_{2z}^{\text{pot}}(x,0)\right\rangle_T = -\frac{U}{\pi}\operatorname{Re}\frac{\partial}{\partial x}\operatorname{arccosh}\left(\cos\left(\frac{\pi x}{T}\right)\Big/\cos\left(\frac{\pi w}{2T}\right)\right). \quad (29)$$

Since the potential φ is an even function of the z coordinate. The component E_{1z}^{pot} on the lower side of the strip conductor is different from the components E_{2z}^{pot} only by the sign. Then from formulas (20) and (29) we get

$$\langle\rho(x)\rangle_T = -\varepsilon_0\frac{\varepsilon_1+\varepsilon_2}{\pi}U\operatorname{Re}\frac{\partial}{\partial x}\operatorname{arccosh}\left(\cos\left(\frac{\pi x}{T}\right)\Big/\cos\left(\frac{\pi w}{2T}\right)\right). \quad (30)$$

Hence, by formula (27), we find the average longitudinal current

$$\langle J_x(x)\rangle_T = -i\omega\varepsilon_0\frac{\varepsilon_1+\varepsilon_2}{\pi}U\operatorname{Re}\operatorname{arccosh}\left(\cos\left(\frac{\pi x}{T}\right)\Big/\cos\left(\frac{\pi w}{2T}\right)\right), \quad (31)$$

and by formula (23), we find the averaged magnetic field

$$\left\langle H_{2y}^{\text{vort}}(x,0)\right\rangle_T = i\omega\varepsilon_0\frac{\varepsilon_1+\varepsilon_2}{2\pi}U\operatorname{Re}\operatorname{arccosh}\left(\cos\left(\frac{\pi x}{T}\right)\Big/\cos\left(\frac{\pi w}{2T}\right)\right). \quad (32)$$

Substituting expression (31) into integral (24), we find the amplitude of the magnetic field

$$H_{2y}^{00} = i\omega\varepsilon_0\frac{\varepsilon_1+\varepsilon_2}{2\pi}U\ln\left(\sec\left(\frac{\pi w}{2T}\right)\right), \quad (33)$$

where the value of the integral was taken into account:

$$\int_{\xi=-a}^{a}\operatorname{arccosh}\left(\frac{\cos\xi}{\cos a}\right)d\xi = \pi\ln(\sec a). \quad (34)$$

In order to find the contribution of the vortex part of the electric field E_x^{vort}, in the mean value $\left\langle E_x^{\text{vort}}\right\rangle_{TT}$, we need to know the component of the magnetic field H_z^{vort}, with which E_x^{vort} is connected by Maxwell's equation

$$(\operatorname{curl}\vec{E}^{\text{vort}})_z = i\omega\mu_0 H_z^{\text{vort}}. \quad (35)$$

To do this, we write the averaging formulas for the current $J_x(x,y)$ and magnetic components $H_{2y}^{\text{vort}}(x,y,z)$ by coordinate x:

$$\langle J_x(y)\rangle_T = \frac{1}{T}\int_{x=-w/2}^{T-w/2} J_x(x,y)dx, \quad (36)$$

$$\left\langle H_{2y}^{\text{vort}}(y,z)\right\rangle_T = \frac{1}{T}\int_{x=-w/2}^{T-w/2} H_{2y}^{\text{vort}}(x,y,z)dx. \quad (37)$$

These values are in agreement with the boundary condition (23) and are bound on the surface of the lattice by the equality

$$\langle J_x(y)\rangle_T = -2\left\langle H_{2y}^{\text{vort}}(y,0)\right\rangle_T. \quad (38)$$

Since the average component $\left\langle H_{2y}^{\text{vort}}(y,z)\right\rangle_T$ is independent of coordinate x, the solution of the 2D Laplace equation (11) for the averaged components can be obtained by the method of conformal mappings [16]. This solution is

$$\left\langle H_{2y}^{\text{vort}}(y,z)\right\rangle_T = i\omega\varepsilon_0\frac{\varepsilon_1+\varepsilon_2}{2\pi^2}TU \times\ln\left(\sec(\frac{\pi w}{2T})\right)\operatorname{Re}\frac{\partial}{\partial y}\arcsin\left(\frac{\sin\left(\pi\frac{y+iz}{T}\right)}{\sin\left(\frac{\pi w}{2T}\right)}\right). \quad (39)$$

It corresponds to the value of amplitude H_{2y}^{00}, expressed by formula (33). A comparison of formulas (32) and (39) allows us to build the function

$$H_{2y}^{\text{vort}}(x,y,0) = i\omega\varepsilon_0\frac{\varepsilon_1+\varepsilon_2}{2\pi^2}TU \times\operatorname{Re}\operatorname{arccosh}\left(\frac{\cos(\pi x/T)}{\cos(\pi w/2T)}\right) \times\operatorname{Re}\frac{\partial}{\partial y}\arcsin\left(\frac{\sin(\pi y/T)}{\sin(\pi w/2T)}\right), \quad (40)$$

which describes the dependency of the component H_{2y}^{vort} from coordinates x and y on the entire surface of the lattice. It is seen that the component H_{2y}^{vort} is not zero only on the surface of the metal patch. The resulting component $H_{2y}^{\text{vort}}(x,y,0)$, according to the boundary condition (23), corresponds to the longitudinal current

$$J_x(x,y) = -i2\omega\varepsilon_0\frac{\varepsilon_1+\varepsilon_2}{2\pi^2}TU \times\operatorname{Re}\operatorname{arccosh}\left(\frac{\cos(\pi x/T)}{\cos(\pi w/2T)}\right) \times\operatorname{Re}\frac{\partial}{\partial y}\arcsin\left(\frac{\sin(\pi y/T)}{\sin(\pi w/2T)}\right). \quad (41)$$

The same current $J_y(x, y)$ can be calculated from the charge conservation law (21); however, in addition to the longitudinal current $J_x(x, y)$, we also we need to know the density of surface charges $\rho(x, y)$. Therefore, we approximate the unknown function $\rho(x, y)$ by the function $\langle\rho(x)\rangle_w$, obtained by averaging $\rho(x, y)$ by coordinate y. Unlike the function $\langle\rho(x)\rangle_T$, given by formula (26), we will not average over the lattice period T but instead over the width of strip w. From formula (30) we get

$$\begin{gathered}\langle\rho(x)\rangle_w = -\frac{T}{w}\varepsilon_0\frac{\varepsilon_1+\varepsilon_2}{\pi} \\ \times U\,\mathrm{Re}\frac{\partial}{\partial x}\operatorname{arccosh}\left(\cos\left(\frac{\pi x}{T}\right)\Big/\cos\left(\frac{\pi w}{2T}\right)\right).\end{gathered} \tag{42}$$

Substituting formulas (41) and (42) into Eq. (21), we find the transverse current

$$\begin{gathered}J_y(x,y) = i\omega\varepsilon_0\frac{\varepsilon_1+\varepsilon_2}{\pi^2}TU \\ \times\mathrm{Re}\frac{\partial}{\partial x}\operatorname{arccosh}\left(\frac{\cos(\pi x/T)}{\cos(\pi w/2T)}\right) \\ \times\mathrm{Re}\left[\arcsin\left(\frac{\sin(\pi y/T)}{\sin(\pi w/2T)}\right)-\frac{\pi y}{w}\right].\end{gathered} \tag{43}$$

Here the integration constant is chosen to be zero so that the current J_y vanished on the edge of the strip conductor when $y = w/2$. According to the boundary condition (23), current J_y corresponds to the component of the magnetic field

$$\begin{gathered}H_{2x}^{\mathrm{vort}}(x,y,0) = i\omega\varepsilon_0\frac{\varepsilon_1+\varepsilon_2}{2\pi^2}TU \\ \times\mathrm{Re}\frac{\partial}{\partial x}\operatorname{arccosh}\left(\frac{\cos(\pi x/T)}{\cos(\pi w/2T)}\right) \\ \times\mathrm{Re}\left[\arcsin\left(\frac{\sin(\pi y/T)}{\sin(\pi w/2T)}\right)-\frac{\pi y}{w}\right].\end{gathered} \tag{44}$$

It meets Meixner's conditions on the edge [22]

$$\begin{gathered}H_x\big|_{|x|\le w/2,\,y=w/2-r} \propto r^{1/2},\quad H_x\big|_{x=w/2-r,\,|y|\le w/2} \propto r^{-1/2}, \\ H_y\big|_{|x|\le w/2,\,y=w/2-r} \propto r^{-1/2},\quad H_y\big|_{x=w/2-\rho,\,|y|\le w/2} \propto r^{1/2}, \\ H_z\big|_{|x|\le w/2,\,y=w/2-r} \propto r^{-1/2}, \\ H_z\big|_{x=w/2-r,\,|y|\le w/2} \propto r^{-1/2}\ (r\to 0).\end{gathered} \tag{45}$$

It is seen that the two components of the magnetic field H_{2x}^{vort} and H_z^{vort} on the edge of the strip conductor between regions I and II have a singularity. This means that near this edge we can neglect the third component H_{2y}^{vort}, and in the Laplace equation (11), we can neglect the derivative components H_{2x}^{vort} and H_z^{vort} by coordinate y compared to the derivatives of the same components by the coordinate x. Then from formula (44), it follows that the component H_z^{vort} in area II can be approximated by the function

$$\begin{gathered}H_z^{\mathrm{II}}(x,y,0) = -i\omega\varepsilon_0\frac{\varepsilon_1+\varepsilon_2}{2\pi^2}TU \\ \times\frac{\partial}{\partial x}\arccos\left(\frac{\cos(\pi x/T)}{\cos(\pi w/2T)}\right) \\ \times\left[\arcsin\left(\frac{\sin(\pi y/T)}{\sin(\pi w/2T)}\right)-\frac{\pi y}{w}\right].\end{gathered} \tag{46}$$

Obviously, such an approximation H_z^{vort} in region II is valid only in the case when the width of this region (T–w) is less than its height w. However, this case is interesting from the point of view of the practical applications of a strip of strip conductors.

At the other end of the conductor, between areas I and IV, according to conditions (45), the singularity contains components H_{2y}^{vort} and H_z^{vort}. Therefore, in region IV of formula (40) and Maxwell's equations

$$\operatorname{div}(\mu_0\vec{H}) = 0 \tag{47}$$

we find the normal component

$$\begin{gathered}H_z^{\mathrm{IV}}(x,y,0) = -i\omega\varepsilon_0\frac{\varepsilon_1+\varepsilon_2}{2\pi^2}TU \\ \times\operatorname{arccosh}\left(\frac{\cos(\pi x/T)}{\cos(\pi w/2T)}\right)\mathrm{Im}\frac{\partial}{\partial y}\arcsin\left(\frac{\sin(\pi y/T)}{\sin(\pi w/2T)}\right).\end{gathered} \tag{48}$$

To find the vortex field $\vec{E}^{\mathrm{vort}}$ in domains II, III, and IV, we turn to Maxwell's equation (35).

In area III, according to formulas (40) and (44), the magnetic components H_{2y}^{vort} and H_{2x}^{vort} are missing; therefore, there will be no third component H_z^{vort} associated with the first two components of Eq. (47). Therefore, in region III, the vortex electric field is $E_x^{\mathrm{III}} = 0$.

In region II, we integrate Eq. (35) by the area bounded by inequalities $w/2 < x < T–w/2$ and $y' < y < w/2$. Using the Stokes rotor theorem, we obtain

$$\begin{gathered}\int\limits_{x=w/2}^{T-w/2} E_x^{\mathrm{II}}(x,y',0)dx \\ = i\omega\mu_0\int\limits_{x=w/2}^{T-w/2}\int\limits_{y=y'}^{w/2} H_z^{\mathrm{II}}(x,y,0)dydx,\end{gathered} \tag{49}$$

where we took into account that on the edges of the conductors, i.e., at $x = w/2$ and $x = T - w/2$, component $E_y^{\mathrm{II}} = 0$, and on the border of regions II and III

$E_x^{\rm II} = 0$. Equation (49) after substitution of expression (46) into it takes the form

$$\int_{x=w/2}^{T-w/2} E_x^{\rm II}(x,y,0)dx = \omega^2\varepsilon_0\mu_0 \frac{\varepsilon_1+\varepsilon_2}{2\pi^2} T^2 U\left[I\left(\frac{\pi y}{T},\frac{\pi w}{2T}\right)+\pi^2\frac{4y^2-w^2}{8wT}\right], \tag{50}$$

where the function $I(\zeta, a)$ denotes the integral

$$I(\zeta,a) = \int_{\xi=\zeta}^{a} \arcsin\left(\frac{\sin\xi}{\sin a}\right)d\xi. \tag{51}$$

In order to find the contribution of $\left\langle E_x^{\rm II}\right\rangle_{TT}$ in amplitude E_x^{00} from components $E_x^{\rm vort}$ on section II, we substitute expression (50) in formula (13). After integration we have

$$\left\langle E_x^{\rm II}\right\rangle_{TT} = \omega^2\varepsilon_0\mu_0\frac{\varepsilon_1+\varepsilon_2}{\pi^3}TU\left[X\left(\frac{\pi w}{2T}\right)-\frac{\pi^3 w^2}{24T^2}\right]. \tag{52}$$

Here the function $X(a)$ denotes the double integral

$$X(a) = \int_{\zeta=0}^{a}\left[\int_{\xi=\zeta}^{a}\arcsin\left(\frac{\sin\xi}{\sin a}\right)d\xi\right]d\zeta. \tag{53}$$

In region IV, we integrate Eq. (35) by the area bounded by inequalities $|x| < w/2$ and $w/2 < y < y'$. Using the Stokes rotor theorem, we obtain

$$-\int_{x=-w/2}^{w/2} E_x^{\rm IV}(x,y',0)dx = i\omega\mu_0\int_{x=-w/2}^{w/2}\int_{y=w/2}^{y'} H_z^{\rm IV}(x,y,0)dydx, \tag{54}$$

where we took into account that on the edge of the strip conductor, i.e., at $y = w/2$, component $E_y^{\rm IV} = 0$, and on the border of regions III and IV we also took into account component $E_x^{\rm IV} = 0$. The equation (54), after substituting expression (48) into it, takes the form

$$-\int_{x=-w/2}^{w/2} E_x^{\rm IV}(x,y',0)dx = \omega^2\varepsilon_0\mu_0\frac{\varepsilon_1+\varepsilon_2}{2\pi^2}T^2U \times \ln\left(\sec\left(\frac{\pi w}{2T}\right)\right)\operatorname{arccosh}\left(\frac{\sin(\pi y'/T)}{\sin(\pi w/2T)}\right). \tag{55}$$

In order to find the contribution of $\left\langle E_x^{\rm IV}\right\rangle_{TT}$ in amplitude E_x^{00} from components $E_x^{\rm vort}$ on section IV, we substitute expression (55) in formula (13). After integration we get

$$\left\langle E_x^{\rm IV}\right\rangle_{TT} = -\omega^2\varepsilon_0\mu_0\frac{\varepsilon_1+\varepsilon_2}{2\pi^2} \times TU\ln\left(\sec\left(\frac{\pi w}{2T}\right)\right)\ln\left(\operatorname{cosec}\left(\frac{\pi w}{2T}\right)\right), \tag{56}$$

where the value of the integral was taken into account:

$$\int_{\xi=a}^{\pi-a}\operatorname{arccosh}\left(\frac{\sin\xi}{\sin a}\right)d\xi = \pi\ln(\operatorname{cosec} a). \tag{57}$$

Summing up the contributions $\left\langle E_x^{\rm pot}\right\rangle_{TT}$, $\left\langle E_x^{\rm II}\right\rangle_{TT}$, and $\left\langle E_x^{\rm IV}\right\rangle_{TT}$, expressed by formulas (19), (52), and (56), we find

$$E_x^{00} = \frac{U}{T}\left[1-\omega^2\varepsilon_0\mu_0\frac{\varepsilon_1+\varepsilon_2}{2\pi^2}T^2\times \times\left[\ln\left(\sec\left(\frac{\pi w}{2T}\right)\right)\ln\left(\operatorname{cosec}\left(\frac{\pi w}{2T}\right)\right) + \frac{\pi^2 w^2}{12T^2}-\frac{2}{\pi}X\right]\left(\frac{\pi w}{2T}\right)\right]. \tag{58}$$

Formulas (33) and (58) for amplitudes H_{2y}^{00} and E_x^{00} allow us to proceed to the direct calculation of the scattering matrix.

2. FORMULAS FOR SCATTERING MATRIX

Calculate the scattering matrix $\mathbf{S}$, considering the surfaces on both sides of the lattice as two ports of a quadrupole. This matrix relates the normalized amplitudes of the scattered waves. b_1 and b_2 emanating from the first and second ports with the normalized amplitudes of the incident waves a_1 and a_2 by the equation [23]

$$\begin{pmatrix} b_1 \\ b_2\end{pmatrix} = \mathbf{S}\begin{pmatrix} a_1 \\ a_2\end{pmatrix}. \tag{59}$$

The normalized amplitudes themselves are determined by the formulas [23]

$$a_{1,2} = E_{1,2}^{\rm inc}\Big/\sqrt{Z_{1,2}},\quad b_{1,2} = E_{1,2}^{\rm sc}\Big/\sqrt{Z_{1,2}}, \tag{60}$$

where $E_{1,2}^{\rm inc}$ are the amplitudes of the incident waves in formula (1), while $E_{1,2}^{\rm sc}$ are the amplitudes of scattered waves.

We write the boundary conditions for the electric field E_x and magnetic field H_y in the first port

$$\begin{aligned} a_1\sqrt{Z_1} + b_1\sqrt{Z_1} &= E_x^{00}, \\ a_1\Big/\sqrt{Z_1} - b_1\Big/\sqrt{Z_1} &= H_{1y}^{00} + H_0. \end{aligned} \tag{61}$$

In Eq. (61) it is taken into account that the wave with amplitude b_1 extends against the direction of the z axis and therefore the magnetic field of this wave is different.

Similar equations are written for the electric and magnetic fields at the second port.

$$\begin{aligned} b_2\sqrt{Z_2} + a_2\sqrt{Z_2} &= E_x^{00}, \\ b_2/\sqrt{Z_2} - a_2/\sqrt{Z_2} &= H_{2y}^{00} + H_0. \end{aligned} \tag{62}$$

Note that the wave with amplitude a_2 extends against the direction of the z axis; therefore, the intensity of its magnetic field has the opposite sign, just as for the wave with amplitude b_1 in the formula (61).

Jointly solving Eqs. (61) and (62) and taking into account that amplitudes H_{1y}^{00} and H_{2y}^{00} differ only in sign, we find the normalized amplitudes of the scattered waves

$$\begin{aligned} b_1 &= \frac{\sqrt{\varepsilon_1} - \sqrt{\varepsilon_2} - Z_0/Z^{\text{lat}}}{\sqrt{\varepsilon_1} + \sqrt{\varepsilon_2} + Z_0/Z^{\text{lat}}} a_1 \\ &+ \frac{2\sqrt[4]{\varepsilon_1\varepsilon_2}}{\sqrt{\varepsilon_1} + \sqrt{\varepsilon_2} + Z_0/Z^{\text{lat}}} a_2, \\ b_2 &= \frac{2\sqrt[4]{\varepsilon_1\varepsilon_2}}{\sqrt{\varepsilon_1} + \sqrt{\varepsilon_2} + Z_0/Z^{\text{lat}}} a_1 \\ &+ \frac{\sqrt{\varepsilon_2} - \sqrt{\varepsilon_1} - Z_0/Z^{\text{lat}}}{\sqrt{\varepsilon_1} + \sqrt{\varepsilon_2} + Z_0/Z^{\text{lat}}} a_2, \end{aligned} \tag{63}$$

where the entered value $Z^{\text{lat}} = E_x^{00}/\left(2H_{1y}^{00}\right)$, which according to formulas (33) and (58) takes the value

$$\begin{aligned} Z^{\text{lat}} &= \frac{i}{\omega\varepsilon_0 \dfrac{\varepsilon_1 + \varepsilon_2}{\pi} T \ln\left(\sec(\frac{\pi w}{2T})\right)} \\ &- i\omega\mu_0 T\left[\frac{1}{2\pi}\ln\left(\operatorname{cosec}(\pi w/2T)\right)\right. \\ &+ \left.\frac{\pi w^2/24T^2 - \pi^{-2}X(\pi w/2T)}{\ln\left(\sec(\pi w/2T)\right)}\right]. \end{aligned} \tag{64}$$

From Eqs. (63) we get the desired scattering matrix

$$\mathbf{S} = \begin{pmatrix} \dfrac{\sqrt{\varepsilon_1} - \sqrt{\varepsilon_2} - Z_0/Z^{\text{lat}}}{\sqrt{\varepsilon_1} + \sqrt{\varepsilon_2} + Z_0/Z^{\text{lat}}} & \dfrac{2\sqrt[4]{\varepsilon_1\varepsilon_2}}{\sqrt{\varepsilon_1} + \sqrt{\varepsilon_2} + Z_0/Z^{\text{lat}}} \\ \dfrac{2\sqrt[4]{\varepsilon_1\varepsilon_2}}{\sqrt{\varepsilon_1} + \sqrt{\varepsilon_2} + Z_0/Z^{\text{lat}}} & \dfrac{\sqrt{\varepsilon_2} - \sqrt{\varepsilon_1} - Z_0/Z^{\text{lat}}}{\sqrt{\varepsilon_1} + \sqrt{\varepsilon_2} + Z_0/Z^{\text{lat}}} \end{pmatrix}. \tag{65}$$

Note that the value Z^{lat} is the impedance of the lattice unit cell. The first term in formula (64), which is inversely proportional to frequency ω, describes the capacitive component of the impedance. The second term, proportional ω, describes the inductive component of the impedance. In this case, the first term of the inductive part of the impedance is due to the longitudinal currents J_x, and the second term is proportional to the transverse currents J_y.

The matrix elements **S** are bound by equalities $S_{12} = S_{21}$ and $|S_{11}| = |S_{22}|$. The first equality indicates that the lattice in question is a mutual quadrupole. Formula (65) exactly matches the formula for the scattering matrix of waves at the junction of the transmission lines with wave impedances Z_1 and Z_2 expressed by formula (3) when this joint is loaded on a parallel oscillating circuit with impedance Z^{lat}.

3. ANALYSIS OF THE OBTAINED FORMULAS

We analyze formula (64). In accordance with the points discussed above, it can be written as

$$Z^{\text{lat}} = \frac{i}{\omega C} - i\omega\left(L_x + L_y\right), \tag{66}$$

where

$$C = \varepsilon_0 \frac{\varepsilon_1 + \varepsilon_2}{\pi} T \ln\left(\sec\left(\frac{\pi w}{2T}\right)\right) \tag{67}$$

is the capacity of the unit cell of the lattice,

$$L_x = \frac{\mu_0 T}{2\pi}\ln\left(\operatorname{cosec}\left(\frac{\pi w}{2T}\right)\right) \tag{68}$$

is the first part of the inductance of the unit cell associated with the longitudinal current J_x, and

$$L_y = \mu_0 T \frac{\pi w^2/24T^2 - \dfrac{1}{\pi^2}X(\pi w/2T)}{\ln\left(\sec(\pi w/2T)\right)} \tag{69}$$

is the second part of the inductance of the elementary cell associated with the transverse current J_y.

In Fig. 2, the capacity dependences C and inductances L_x and L_y of the unit cell lattice on width w of its strip conductors are constructed. These dependences are calculated by formulas (65)–(69) for lattices with period T = 3 mm, located at the interface of media with dielectric constant $\varepsilon_1 = 1$ and $\varepsilon_2 = 2$. It can be seen that with the width of conductors w increasing from zero to T, capacity C grows from zero to infinity, inductance L_x, corresponding to the longitudinal currents, decreases from infinity to zero, and inductance L_y, corresponding to transverse currents, decreases to zero from some final value. However, as noted, the validity of the approximation used in the calculation is determined by the following condition: the width of region II (see Fig. 1) (T–w) must be less than its height w. The zone where this condition is not fulfilled is indicated in Fig. 2 in gray.

The dependence of the ratio of the transverse part of inductance L_y to the complete inductance $L_x + L_y$ on the relative width of conductors w/T is presented in Fig. 3. This ratio does not depend on period T nor on the dielectric constant of the media between which the

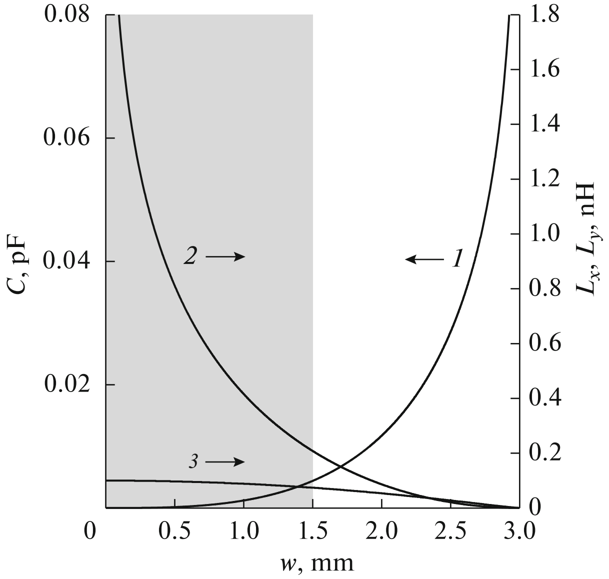

Fig. 2. Capacity dependences C (*1*), and longitudinal L_x (*2*) and transverse L_y (*3*) inductances of elementary lattice cell from width of its conductors during lattice period $T = 3$ mm.

lattice is located. It can be seen that it always grows with an increase in the width of the strip conductor and approaches unity at $w \to T$. The zone where the condition for the validity of the approximation used in the calculation is not satisfied is also marked with a gray background.

We built the frequency dependences of the reflection coefficient $|S_{11}|^2$ and the coefficient of the passage $|S_{21}|^2$ of the electromagnetic wave through a lattice on the interface between media and dielectric constant $\varepsilon_1 = 1$ and $\varepsilon_2 = 2$ according to formulas (53), (64), and (65) (Fig. 4). These dependences are calculated for several widths w of the conductors with a fixed lattice period of $T = 3$ mm. It is seen that the reflection coefficient $|S_{11}|^2$ grows as the frequency increases and also as the width of the strip conductors increases.

In order to estimate the error of the formulas obtained, we performed a numerical electrodynamic calculation of a 3D model of a square strip conductor grid in the CST Microwave Studio software package. It was assumed that the conductors have infinite conductivity and zero thickness. A comparison of the matrix elements calculated by the formulas and obtained using a software package was made for the grid of conductors located at the interface between media with dielectric constants $\varepsilon_1 = 1$ and $\varepsilon_2 = 2$ having a period of $T = 3$ mm. Numerical calculations of the 3D model showed that for the lattices considered the lowest resonant frequency at which the transmission coefficient $|S_{21}|^2$ vanishes is approximately 70 GHz. However, in the region of such high frequencies, the conditions of the quasi-static approximation are not satisfied; therefore, the formulas obtained here can no longer be used.

In Fig. 5, the frequency dependences of the relative errors in the calculation of the elements of the scattering matrix are presented for three strip widths w. The

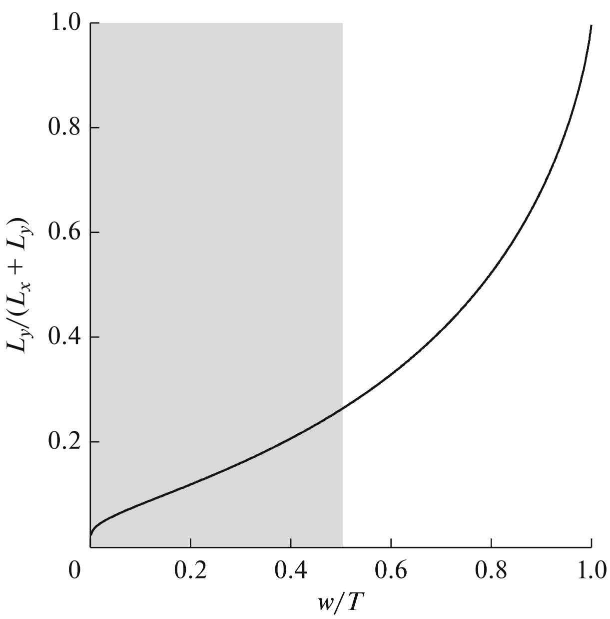

Fig. 3. Dependence of ratio of transverse part of inductance to total inductance on relative width of strip conductors of lattice.

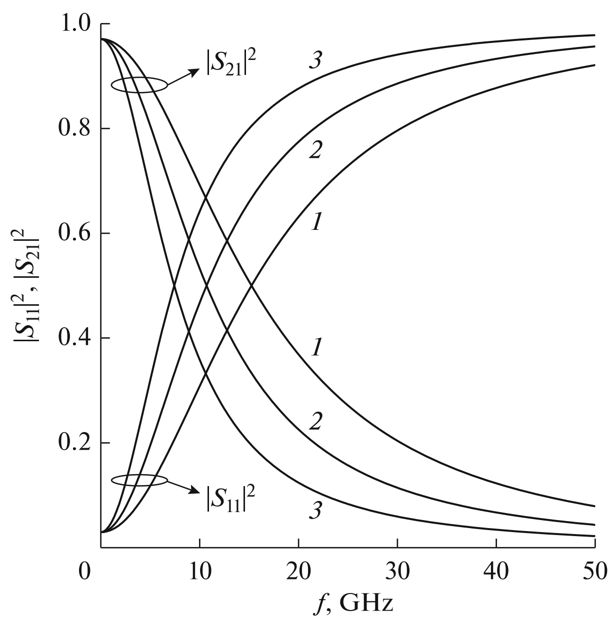

Fig. 4. Frequency dependence of reflection coefficients $|S_{11}|^2$ and transmission $|S_{21}|^2$ for lattice with period $T = 3$ mm and conductor width $w = 2.85$ (*1*), 2.95 (*2*), 2.99 mm (*3*).

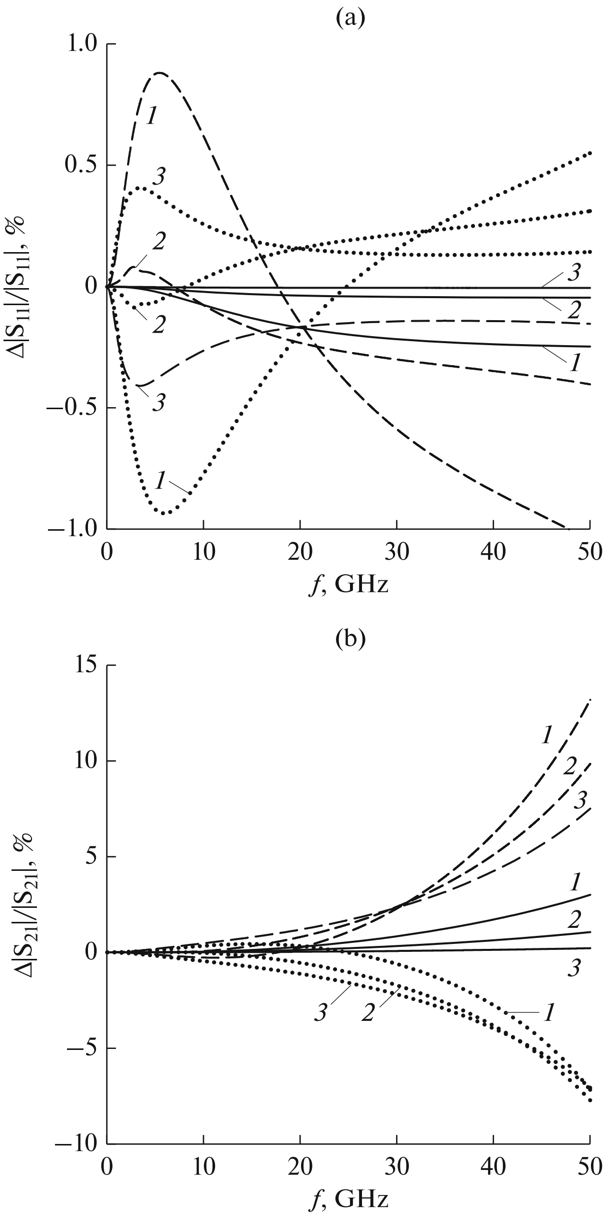

Fig. 5. Frequency dependences of relative error in calculation of elements of scattering matrix S_{11} (a) and S_{21} (b) for three values of width of strip conductor, w = 2.85 (*1*), 2.95 (*2*), 2.99 mm (*3*); dashed lines are calculation by known formulas, dotted lines are calculation by obtained formulas (65)–(69); solid lines obtained using averaged formula (71).

dotted lines represent the calculation error using the formulas (65)–(69) obtained. The dashed lines represent the calculation error using the well-known formula [12, 24]

$$Z^{\text{lat}} = \frac{i}{\omega\varepsilon_0 \dfrac{\varepsilon_1 + \varepsilon_2}{\pi} T \ln\left(\sec\left(\dfrac{\pi w}{2T}\right)\right)} \qquad (70)$$

if we substitute it in formula (65) to calculate the scattering matrix of electromagnetic waves on the capacitive lattice of strip conductors. This formula differs from formula (66) only by the absence of inductance L_x and L_y. As we can see, the difference between the dotted and dashed lines lies primarily in the opposite signs of the errors they display. Therefore, instead of the resulting formula (66), we suggest using the averaged formula

$$Z^{\text{lat}} = \frac{i}{\omega C} - i\omega\frac{L_x + L_y}{2} \qquad (71)$$

with the same values of electrical parameters C, L_x, and L_y. The error in calculating the scattering matrix when using the averaged formula (71) is also shown in Fig. 5. This error is smaller by many factors than the error obtained by using formulas (66) or (70).

CONCLUSIONS

The solution of Maxwell's equations, obtained in the work in the quasi-static approximation, confirms the fact that the lattice of strip conductors at the interface of two media is equivalent to a series oscillatory circuits connected in parallel to the cascade points of two transmission lines. The values of the elements of the scattering matrix of such a lattice depend only on the impedance Z^{lat} of its unit cell, which is determined by the topology of the strip conductors and the dielectric constant of media ε_1 and ε_2. Impedance Z^{lat}, according to formula (66), is the sum of two parts that differ in frequency dependence. Its capacitive part decreases in absolute value in inverse proportion to frequency ω, and the inductive part grows in absolute value in direct proportion to ω. This means that at low frequencies the capacitive part Z^{lat} prevails in absolute value over the inductive part. Therefore, at sufficiently low frequencies, the inductance of the unit cell can be neglected in comparison with its capacity, expressed by formula (67).

Formula (67) confirms the empirical hypothesis [13, 21] about the coincidence at low frequencies of the reflective properties of a subwave lattice of square strip conductors and the strip travel of strip conductors in the case of a linearly polarized electromagnetic wave falling on it with the direction of the electric field vector orthogonal to the strip conductors. In this case, both grids must have the same period, and the width of the strip conductors must be equal to the size of the side of the square conductors.

However, with increasing frequency, it is necessary to consider not only the capacitive but also the inductive part of the impedance Z^{lat} due to both the longitudinal J_x and transverse J_y current components in the square strip conductors. The inductive part of an impedance is characterized by the sum of the corresponding inductances L_x and L_y described by formulas (68) and (69), which were obtained for the first time. A comparison of the frequency characteristics calculated by the formulas and obtained by the numerical electrodynamic calculation of the 3D model of the structure under consideration showed that taking the inductive part of the impedance into account allows us to repeatedly increase the accuracy of the calculation at high frequencies.

It is important to note that the structure studied can be used to create mirrors with the given reflectivity at the interfaces of the dielectric layers. Such mirrors are necessary when designing optical and microwave multilayer band-pass filters or radio-transparent surfaces in a given frequency range in order to hide antennas. In this case, the lattices of the square strip conductors at the boundaries of the dielectric layers of the resonators make it possible to ensure the optimal connections between the resonators with each other, and of the resonators on the edges with space. The similarity of such filters is demonstrated by their similar multilayer structures, but with the lattices in the form of metal grids at the interfaces of the dielectric layers [19]. Using the formulas derived in [20] for metal grids, and the formulas obtained in this work for square metal conductor lattices, will allow us to significantly reduce the design time of frequency selective devices on multilayer dielectric structures.

FUNDING

The study was supported by the Ministry of Education and Science of the Russian Federation (agreement no. 14.575.21.0279, unique project identifier RFMEFI57517X0142).

REFERENCES

1. B. A. Belyaev and V. V. Tyurnev, Microw. Opt. Technol. Lett. **55**, 1613 (2013).
2. H. A. Macleod, *Thin-film Optical Filters* (CRC, Boca Raton, 2010).
3. B. A. Belyaev, V. V. Tyurnev, and V. F. Shabanov, Dokl. Phys. **59**, 73 (2014).
4. B. A. Belyaev, V. V. Tyurnev, and V. F. Shabanov, Dokl. Phys. **59**, 245 (2014).
5. B. A. Belyaev, V. V. Tyurnev, and V. F. Shabanov, Opt. Lett. **39**, 3512 (2014).
6. P. A. R. Ade, G. Pisano, C. Tucker, and S. Weaver, Proc. SPIE **6275**, 62750 (2006).
7. A. M. Melo, M. A. Kornberg, P. Kaufmann, et al., Appl. Opt. **47**, 6064 (2008).
8. F. J. Garcia-Vidal, L. Martin-Moreno, T. W. Ebbesen, and L. Kuipers, Rev. Mod. Phys. **82**, 729 (2010).
9. B. Munk, *Frequency Selective Surfaces: Theory and Design* (Wiley, New York, 2000).
10. P. Tomasek, Int. J. Circuits, Systems & Signal Processing **8**, 594 (2014).
11. S. Oh, H. Lee, J-H. Jung, and G-Y. Lee, Int. J. Microwave Sci. Technol. **2014**, 857582 (2014).
12. M. A. Al-Joumayly and N. Behdad, IEEE Trans. Antennas Propag. **58**, 4030 (2010).
13. R. Ulrich, Infrared Phys. **7**, 37 (1967).
14. B. A. Belyaev and V. V. Tyurnev, Opt. Lett. **40**, 4333 (2015).
15. B. A. Belyaev and V. V. Tyurnev, Opt. Lett. **41**, 536 (2016).
16. B. A. Belyaev and V. V. Tyurnev, Izv. Vyssh. Uchebn. Zaved. Fiz. **58**, 57 (2015).
17. S. E. Bankov and I. V. Levchenko, Radiotekh. Elektron. (Moscow) **33**, 2045 (1988).
18. B. A. Belyaev and V. V. Tyurnev, Microw. Opt. Technol. Lett. **60**, 630 (2018).
19. B. A. Belyaev, V. V. Tyurnev, A. S. Voloshin and R. G. Galeev, Tech. Phys. Lett. **44**, 408 (2018).
20. B. A. Belyaev and V. V. Tyurnev, J. Commun. Technol. Electron. **62**, 750 (2017).
21. L. B. Whitbourn and R. C. Compton, Appl. Opt. **24** (2), 217 (1985).
22. J. Meixner, IEEE Trans. Antennas Propag. **20**, 442 (1972).
23. K. C. Gupta, R. Garg, and R. Chadha, *Computer-Aider Design of Microwave Circuits* (Artech House, Dedham, MA, 1981; Radio i Svyaz', Moscow, 1987).
24. O. Luukkonen, C. Simovski, G. Granet et al., IEEE Trans. **AP-56** (6), 1624 (2008).